

Lossless/lossy Image Compression based on Non-Separable Two-Dimensional LWT

Somchart CHOKCHAITAM¹ and Masahiro IWAHASHI²

¹Department of Electrical Engineering, Faculty of Engineering
Thammasat University, Patoom-Thani, Thailand
E-mail: somchart@tech.nagaokaut.ac.jp

²Department of Electrical Engineering, Faculty of Engineering
Nagaoka University of Technology, Nagaoka city, Niigata, 940-2188, Japan
E-mail: iwahashi@vos.nagaokaut.ac.jp

Abstract

In this report, we propose a non-separable two-dimensional (2D) Lossless Wavelet Transform (LWT) for image compression. Filter characteristics of our proposed LWT are the same as those of conventional 2D LWT based on applying 1D LWT twice but our coding performance is better due to reduction of rounding effects. Simulation results confirm effectiveness of our proposed LWT.

Key words: LWT, non-separable, two-dimensional, filter bank, rounding effect, image compression

1. Introduction

Many researchers have been paying attention to lossless algorithm to serve some applications that require a high-quality decoded image such as medical image. The Lossless Wavelet Transform (LWT) [1] is one of the famous lossless algorithms because the LWT-based coding system can provide not only lossy coding but also lossless coding thanks to lifting structures (LS) and rounding operations. However, the error generated from rounding operation [2] causes PSNR degradation in lossy coding when quantization is applied. The conventional LWT is a one-dimensional (1D) filter bank (FB) constructed from double LS. To perform 2D FB for image application, the 1D LWT is applied twice in horizontal and vertical dimension, successively. Namely, it is a separable 2D LWT.

In this report, we propose a non-separable 2D LWT. The number of rounding operations of our proposed LWT is less than that of conventional 2D LWT, whereas filter characteristics of our proposed LWT are the same as those of conventional 2D LWT when error generated by the rounding operation is negligible. Therefore, coding performance of our proposed LWT is better than that of the conventional 2D LWT in lossy coding, especially at high bit rate when quantization errors are relatively small compared to the rounding errors. Moreover, coding performance of our proposed LWT is slightly better than that of the conventional 2D LWT in lossless coding.

This report is organized as follows. We review signal processing of the conventional 2D LWT in section 2. Then, we propose a new signal processing of non-separable 2D LWT for image compression in section 3. Theoretical analysis confirms advantages of a new signal processing in section 4. Simulation results confirm effectiveness of our proposed LWT in both lossless coding and lossy coding in section 5. Finally, we summarize our proposed LWT in section 6.

2. Signal Processing of the Conventional Two-Dimensional (2D) LWT

The conventional 2D LWT is constructed by applying conventional 1D LWT in horizontal and vertical direction independently as illustrated in figure 1. Input signal (X) is decomposed into 4 subbands (Y_{LL} , Y_{LH} , Y_{HL} , Y_{HH}). For example, Y_{LH} indicates horizontally low-passed and vertically high-passed subband. The z_1 and z_2 denotes horizontal and vertical dimension, respectively. The Q_{LL} , Q_{LH} , Q_{HL} , Q_{HH} denote quantization in subband LL, LH, HL, and HH, respectively. The LS denotes lifting structure. The \textcircled{R} and " $\downarrow 2$ " denote the rounding operation and the down-sampler by two [3]. As shown in figure 1, six rounding operations are required to perform conventional 2D LWT.

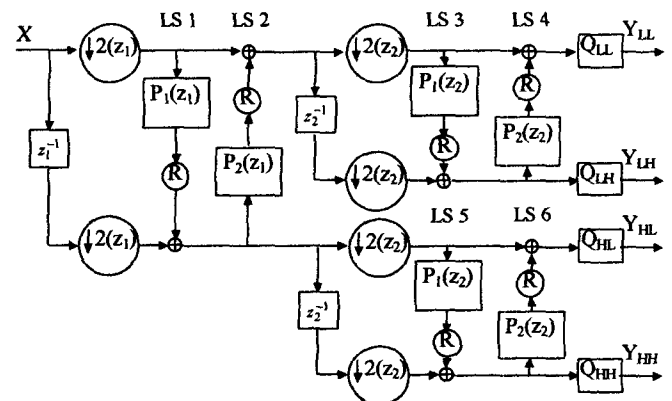


Fig.1 Analysis part of the conventional 2D LWT.

3. Signal processing of the proposed non-separable 2D LWT

In this section, we propose a new 2D LWT with reduced rounding operations. As shown in figure 2, signal processing of our 2D LWT requires only four rounding operations but its filter characteristics are same as those of conventional 2D LWT. Because of advantages of the non-separable 2D FB, parameters in different LS of conventional 2D LWT can be combined. For example, parameters of LS 1 and LS 5 in figure 1 are combined into those of LS 1' in figure 2. Therefore, the number of rounding operations required to perform the 2D LWT is reduced.

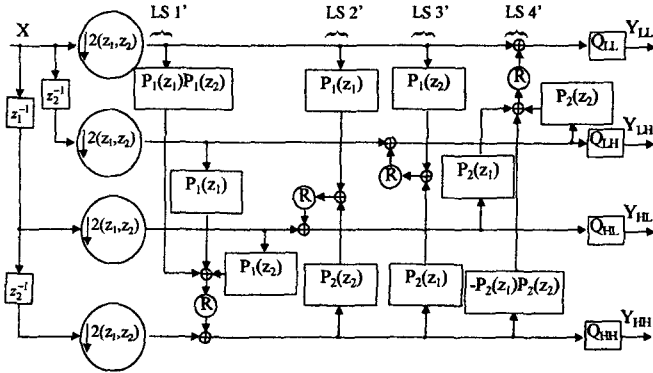


Fig.2 Analysis part of the proposed non-separable 2D LWT.

4. Theoretical Analysis

In this section, we theoretically illustrate advantages of the proposed non-separable 2D LWT. Equivalent expressions of the conventional 2D LWT and the proposed 2D LWT are illustrated in section 4.1 and section 4.2, respectively. Rounding errors of both LWT-based coding systems are analyzed in section 4.3. In this report, we analyze all signal processing under the following assumptions. (1) All filters in this report are linear and time-invariant, and (2) Correlations between each of the errors and the signals are zero (statistical independence). We use the 2D z-transform defined by

$$X(\mathbf{z}) = \sum_{k_1, k_2} x(k_1, k_2) z_1^{-k_1} z_2^{-k_2}, \quad (\mathbf{z}) = (z_1, z_2) \quad (1)$$

where $x(k)$ denotes signal's intensity given in "integer".

4.1 Filter characteristics and the rounding errors of the conventional LWT

Based on the assumptions above, signal processing in figure 1 can be replaced by its equivalent expression in figure 3 where its filter characteristics (H_C) are

$$\begin{bmatrix} H_{LLC}(\mathbf{z}) \\ H_{LHC}(\mathbf{z}) \\ H_{HLC}(\mathbf{z}) \\ H_{HHC}(\mathbf{z}) \end{bmatrix} = \mathbf{T}_{C4}(\mathbf{z})\mathbf{T}_{C3}(\mathbf{z})\mathbf{T}_{C2}(\mathbf{z})\mathbf{T}_{C1}(\mathbf{z}) \begin{bmatrix} 1 \\ z_1^{-1} \\ z_2^{-1} \\ z_1^{-1}z_2^{-1} \end{bmatrix} \quad (2)$$

where transform matrix (\mathbf{T}_{Ci}) are based on parameters of the conventional 2D LWT in figure 1 as

$$\mathbf{T}_{C1}(\mathbf{z}) = \begin{bmatrix} 1 & 0 & 0 & 0 \\ 0 & 1 & 0 & 0 \\ P_1(z_1^2) & 0 & 1 & 0 \\ 0 & P_1(z_1^2) & 0 & 1 \end{bmatrix} \quad (3)$$

$$\mathbf{T}_{C2}(\mathbf{z}) = \begin{bmatrix} 1 & 0 & P_2(z_2^2) & 0 \\ 0 & 1 & 0 & P_2(z_2^2) \\ 0 & 0 & 1 & 0 \\ 0 & 0 & 0 & 1 \end{bmatrix} \quad (4)$$

$$\mathbf{T}_{C3}(\mathbf{z}) = \begin{bmatrix} 1 & 0 & 0 & 0 \\ P_1(z_1^2) & 1 & 0 & 0 \\ 0 & 0 & 1 & 0 \\ 0 & 0 & P_1(z_1^2) & 1 \end{bmatrix} \quad (5)$$

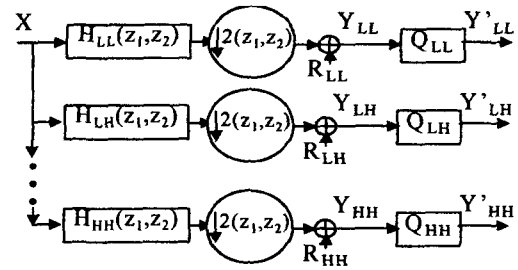


Fig.3 The equivalent expression of the LWT.

$$\mathbf{T}_{C4}(\mathbf{z}) = \begin{bmatrix} 1 & P_2(z_2^2) & 0 & 0 \\ 0 & 1 & 0 & 0 \\ 0 & 0 & 1 & P_2(z_2^2) \\ 0 & 0 & 0 & 1 \end{bmatrix} \quad (6)$$

According to Reichel's report [2], non-linearity of the rounding operation generates additive noise and then the noise is propagated through FB to the reconstructed image. Therefore, denoting the rounding errors as $R_i(z_1, z_2)$ the rounding errors in each band signals can be expressed by

$$\begin{bmatrix} R_{LLC}(\mathbf{z}) & R_{LHC}(\mathbf{z}) & R_{HLC}(\mathbf{z}) & R_{HHC}(\mathbf{z}) \end{bmatrix}^T \\ = \mathbf{R}_{46}(\mathbf{z}) + \mathbf{T}_{C4}(\mathbf{z})\mathbf{R}_{35}(\mathbf{z}) + \mathbf{T}_{C4}(\mathbf{z})\mathbf{T}_{C3}(\mathbf{z})\mathbf{R}_{22}(\mathbf{z}) \\ + \mathbf{T}_{C4}(\mathbf{z})\mathbf{T}_{C3}(\mathbf{z})\mathbf{T}_{C2}(\mathbf{z})\mathbf{R}_{11}(\mathbf{z}) \quad (7)$$

where

$$\mathbf{R}_{46}(\mathbf{z}) = [R_4(\mathbf{z}) \ 0 \ R_6(\mathbf{z}) \ 0]^T$$

$$\mathbf{R}_{35}(\mathbf{z}) = [0 \ R_3(\mathbf{z}) \ 0 \ R_5(\mathbf{z})]^T$$

$$\mathbf{R}_{22}(\mathbf{z}) = [R_2(\mathbf{z}) \ R_2(\mathbf{z}) \ 0 \ 0]^T$$

$$\mathbf{R}_{11}(\mathbf{z}) = [0 \ 0 \ R_1(\mathbf{z}) \ R_1(\mathbf{z})]^T$$

and s additive errors generated from rounding operation in lifting structure i^{th} in figure 1.

4.2 Filter characteristics and the rounding errors of the proposed LWT

Similarly, signal processing in figure 2 can be replaced by its equivalent expression in figure 3 where its filter characteristics (H_P) are

$$\begin{bmatrix} H_{LLP}(\mathbf{z}) \\ H_{LHP}(\mathbf{z}) \\ H_{HLP}(\mathbf{z}) \\ H_{HHP}(\mathbf{z}) \end{bmatrix} = \mathbf{T}_{P4}(\mathbf{z})\mathbf{T}_{P3}(\mathbf{z})\mathbf{T}_{P2}(\mathbf{z})\mathbf{T}_{P1}(\mathbf{z}) \begin{bmatrix} 1 \\ z_1^{-1} \\ z_2^{-1} \\ z_1^{-1}z_2^{-1} \end{bmatrix} \quad (8)$$

where transform matrix (\mathbf{T}_{Pi}) are based on parameters of non-separable 2D LWT in figure 2 as

$$\mathbf{T}_{P1}(\mathbf{z}) = \begin{bmatrix} 1 & 0 & 0 & 0 \\ 0 & 1 & 0 & 0 \\ 0 & 0 & 1 & 0 \\ P_1(z_1^2)P_1(z_2^2) & P_1(z_1^2) & P_1(z_2^2) & 1 \end{bmatrix} \quad (9)$$

$$\mathbf{T}_{P2}(\mathbf{z}) = \begin{bmatrix} 1 & 0 & 0 & 0 \\ 0 & 1 & 0 & 0 \\ P_1(z_1^2) & 0 & 1 & P_2(z_2^2) \\ 0 & 0 & 0 & 1 \end{bmatrix} \quad (10)$$

$$\mathbf{T}_{P3}(\mathbf{z}) = \begin{bmatrix} 1 & 0 & 0 & 0 \\ P_1(z_2^2) & 1 & 0 & P_2(z_1^2) \\ 0 & 0 & 1 & 0 \\ 0 & 0 & 0 & 1 \end{bmatrix} \quad (11)$$

$$\mathbf{T}_{P4}(\mathbf{z}) = \begin{bmatrix} 1 & P_2(z_2^2) & P_2(z_1^2) & -P_2(z_2^2)P_2(z_1^2) \\ 0 & 1 & 0 & 0 \\ 0 & 0 & 1 & 0 \\ 0 & 0 & 0 & 1 \end{bmatrix} \quad (12)$$

Eq. (2) and Eq. (8) confirm that filter characteristics of our proposed non-separable 2D LWT are same as those of the conventional 2D LWT as

$$H_{b,c}(\mathbf{z}) = H_{b,p}(\mathbf{z}) \quad b \in LL, LH, HL, HH \quad (13)$$

The rounding errors in each sub-band of the proposed LWT becomes

$$\begin{aligned} & \left[\mathbf{R}_{LLP}(\mathbf{z}) \quad \mathbf{R}_{LHP}(\mathbf{z}) \quad \mathbf{R}_{HLP}(\mathbf{z}) \quad \mathbf{R}_{HHP}(\mathbf{z}) \right]^T \\ &= \mathbf{R}'_4(\mathbf{z}) + \mathbf{T}_{P4}(\mathbf{z})\mathbf{R}'_3(\mathbf{z}) + \mathbf{T}_{P4}(\mathbf{z})\mathbf{T}_{P3}(\mathbf{z})\mathbf{R}'_2(\mathbf{z}) \\ &+ \mathbf{T}_{P4}(\mathbf{z})\mathbf{T}_{P3}(\mathbf{z})\mathbf{T}_{P2}(\mathbf{z})\mathbf{R}'_1(\mathbf{z}) \end{aligned} \quad (14)$$

where

$$\begin{aligned} \mathbf{R}'_4(\mathbf{z}) &= [\mathbf{R}'_4(\mathbf{z}) \quad 0 \quad 0 \quad 0]^T \\ \mathbf{R}'_3(\mathbf{z}) &= [0 \quad \mathbf{R}'_3(\mathbf{z}) \quad 0 \quad 0]^T \\ \mathbf{R}'_2(\mathbf{z}) &= [0 \quad \mathbf{R}'_2(\mathbf{z}) \quad 0 \quad 0]^T \\ \mathbf{R}'_1(\mathbf{z}) &= [0 \quad 0 \quad 0 \quad \mathbf{R}'_1(\mathbf{z})]^T \end{aligned}$$

where \mathbf{R}'_i denotes rounding errors generated by the rounding operations in the i^{th} lifting structure in figure 2.

4.3 Errors in the decoded image

In this section, we analyze errors in the decoded image of the coding system illustrated in figure 4. Total errors "E" is a sum of the rounding error "R" and the quantization error "Q". Therefore variance of the total errors is

$$\sigma_E^2 = \sigma_Q^2 + \sigma_R^2 \quad (15)$$

Variance of the quantization errors is calculated by

$$\sigma_Q^2 = \frac{\Delta^2}{12} * \frac{1}{4} (\|H_{LL}\|^2 + \|H_{LH}\|^2 + \|H_{HL}\|^2 + \|H_{HH}\|^2) + \frac{1}{12} \quad (16)$$

where Δ denotes quantization step size and the norm is defined by

$$\|H\|^2 = \sum_{k_1, k_2} h^2(k_1, k_2) \quad \text{for } H(z) = \sum_{k_1, k_2} h(k_1, k_2) z_1^{-k_1} z_2^{-k_2} \quad (17)$$

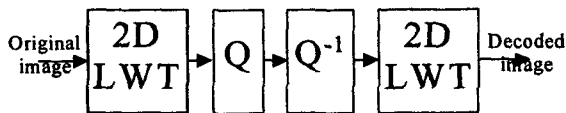


Fig.4 The LWT-based coding system

From equation (7), we can calculate variance of the errors of the conventional system by

$$\sigma_{R,C}^2 = \sum_{i=1}^6 \mathbf{S}_i(\mathbf{z}) (\sigma_{R_{AIC}}^2 + \sigma_{R_{SIC}}^2) \quad (18)$$

where

$$\begin{aligned} \mathbf{S}_1(\mathbf{z}) &= \frac{1}{2}, \quad \mathbf{S}_2(\mathbf{z}) = \frac{1}{2} \|1 - z_1 P_1(z_1^2)\|^2, \quad \mathbf{S}_3(\mathbf{z}) = \frac{1}{4} \|1 - z_1 P_1(z_1^2)\|^2 \\ \mathbf{S}_4(\mathbf{z}) &= \frac{1}{4} \|1 - z_1 P_1(z_1^2)\|^2 \|1 - z_2 P_1(z_2^2)\|^2, \\ \mathbf{S}_5(\mathbf{z}) &= \frac{1}{4} \|1 - z_1^{-1} P_2(z_1^2) + P_1(z_1^2) P_2(z_1^2)\|^2, \\ \mathbf{S}_6(\mathbf{z}) &= \frac{1}{4} \|1 - z_2 P_1(z_2^2)\|^2 \|1 - z_1^{-1} P_2(z_1^2) + P_1(z_1^2) P_2(z_1^2)\|^2 \end{aligned}$$

and $\sigma_{R_s}^2$ and $\sigma_{R_a}^2$ denote variances of the rounding error in analysis part and synthesis part, respectively.

From equation (14), we can calculate variance of the errors of the proposed method by

$$\sigma_{R,P}^2 = \sum_{i=1}^4 \mathbf{S}'_i(\mathbf{z}) (\sigma_{R_{AIP}}^2 + \sigma_{R_{SIP}}^2) \quad (19)$$

where

$$\begin{aligned} \mathbf{S}'_1(\mathbf{z}) &= \frac{1}{4}, \quad \mathbf{S}'_2(\mathbf{z}) = \frac{1}{4} \|1 - z_1 P_1(z_1^2)\|^2, \quad \mathbf{S}'_3(\mathbf{z}) = \frac{1}{4} \|1 - z_1 P_1(z_1^2)\|^2 \\ \mathbf{S}'_4(\mathbf{z}) &= \frac{1}{4} \|1 - z_1 P_1(z_1^2)\|^2 \|1 - z_2 P_1(z_2^2)\|^2 \end{aligned}$$

When we can assume that power spectrum of all errors are flat, variance of the rounding errors become

$$\sigma_{R_{A1}}^2 = \sigma_{R_{A2}}^2 = \dots = \sigma_{R_{A6}}^2 = \sigma_{R_{S1}}^2 = \sigma_{R_{S2}}^2 = \dots = \frac{1}{12} \quad (20)$$

Variances of the errors generated by both the quantization and the rounding operation are theoretically calculated with equations (15)-(20) in the next section.

5. Simulation results

In this section, we apply some standard images as input signals to illustrate effectiveness of our proposed method. Three different kinds of the LWT [1] are used for lossless coding and lossy coding of images in section 5.1 and section 5.2, respectively. Parameters of the LWT including variance of the rounding errors are summarized in Table 1.

Table 1. Parameters of the LWT

LW	$P_1(z)$	$P_2(z)$	$\sigma_{R,C}^2$	$\sigma_{R,P}^2$
T				
5/3	$\frac{(1+z^{-1})}{2}$	$\frac{(z+1)}{4}$	0.43 95	0.26 04
13/ 11- A	$\frac{150(1+z^{-1})}{256} + \frac{25(z+z^{-2})}{256}$ $\frac{25(z^2+z^{-3})}{256}$	$\frac{(z+1)}{4}$	0.49 19	0.30 51
13/ 7-T	$\frac{9(1+z^{-1})}{16} + \frac{(z+z^{-2})}{16}$	$\frac{9(z+1)}{32}$ $\frac{(z^2+z^{-1})}{32}$	0.47 26	0.29 05

5.1 Effectiveness of the proposed method in lossless coding

Table 2 and Table 3 illustrate lossless coding performance of both LWT in term of the entropy rate calculated by

$$H = - \sum_s P_s \log_2 P_s \quad (21)$$

where P_s indicates probability of a symbol "s". The "proposed" and "conventional" indicate "proposed non-separable 2D LWT" and "the conventional 2D LWT", respectively. Table 2 and table indicate that entropy rates of the proposed method are slightly less than those of the conventional one.

Table 2. Entropy rate in lossless coding of the proposed LWT

Image name	5/3	13/11-A	13/7-T
Couple	4.7401	4.7586	4.7431
Aerial	5.932	5.9075	5.9001
Girl	5.1248	5.1231	5.1097
Mobile	5.3377	5.371	5.3519
Barbara	5.5157	5.3721	5.3958

Table 3. Entropy rate in lossless coding of the conventional LWT

Image name	5/3	13/11-A	13/7-T
Couple	4.7484	4.7684	4.752
Aerial	5.9331	5.9093	5.9013
Girl	5.1283	5.124	5.1121
Mobile	5.3397	5.372	5.3536
Barbara	5.5171	5.3767	5.4019

5.2 Effectiveness of proposed method in lossy coding

Table 4-7 illustrate lossy coding performance of both methods in term of PSNR (Peak Signal to Noise Ratio) defined as

$$PSNR = 10 \log_{10} \left(\frac{255^2}{\sigma_E^2} \right) [dB] \quad (22)$$

From results in Table 4-7, PSNR of our LWT are higher than those of conventional 2D LWT with both practical simulation and theoretical calculation, especially in high bit rate when quantization errors are small.

Table 4. PSNR at total bit rate = 4 bpp of the proposed LWT (Practical / Theoretical)

Image name	5/3	13/11-A	13/7-T
Couple	49.29 / 50.13	48.75 / 49.55	48.85 / 49.79
Aerial	45.41 / 45.49	44.96 / 45.07	45.14 / 45.33
Girl	48.89 / 48.93	47.95 / 48.40	48.19 / 48.66
Mobile	47.20 / 48.13	46.16 / 47.46	46.42 / 47.76
Barbara	46.11 / 47.41	46.37 / 47.46	46.41 / 47.58

Table 5. PSNR at total bit rate = 3 bpp of the proposed LWT (Practical / Theoretical)

Image name	5/3	13/11-A	13/7-T
Couple	46.31 / 45.91	45.70 / 45.78	45.90 / 46.07
Aerial	40.01 / 40.00	39.53 / 39.72	39.81 / 40.01
Girl	44.48 / 44.19	43.75 / 43.99	44.08 / 44.29
Mobile	43.09 / 43.15	42.28 / 42.69	42.73 / 43.03
Barbara	42.27 / 42.24	42.08 / 42.68	42.21 / 42.80

Table 6. PSNR at total bit rate = 4 bpp of the conventional LWT (Practical / Theoretical)

Image name	5/3	13/11-A	13/7-T
Couple	48.92 / 49.03	48.38 / 48.53	48.46 / 48.75
Aerial	45.08 / 45.08	44.62 / 44.67	44.85 / 44.93
Girl	48.11 / 48.07	47.60 / 47.61	47.12 / 47.84
Mobile	46.61 / 47.41	45.78 / 46.81	46.01 / 47.08
Barbara	45.78 / 46.78	46.07 / 46.80	46.08 / 46.91

Table 7. PSNR at total bit rate = 3 bpp of the conventional LWT (Practical / Theoretical)

Image name	5/3	13/11-A	13/7-T
Couple	45.99 / 45.87	45.37 / 45.29	45.58 / 45.57
Aerial	39.89 / 39.99	39.46 / 39.60	39.71 / 39.88
Girl	44.18 / 44.18	43.61 / 43.68	43.78 / 43.96
Mobile	42.87 / 43.15	42.08 / 42.46	42.44 / 42.78
Barbara	42.08 / 42.23	41.91 / 42.43	42.03 / 42.54

6. Conclusion

In this report, we proposed a non-separable 2D LWT with fewer rounding operations. The coding performance of our proposed method is better than that of the conventional 2D LWT because the proposed LWT has less number of rounding operations required to perform 2D filter bank, however filter characteristics of both methods are exactly same. Simulation results confirm effectiveness of our proposed method in lossy coding at high bit-rate, additionally in lossless coding.

Computational load of the proposed non-separable 2D LWT is increased comparing to that of the conventional one.

References

- [1] S. Chokchaitam, M. Iwahashi, P. Zavorsky, N. Kambayashi, "Lossless Coding Gain and Its Application to Evaluation of Lossless Wavelets," IEEE ISPACS'00, Nov. 2000.
- [2] J. Reichel, G. Menegaz, M. J. Nadenau, M. Kunt, "Integer Wavelet Transform for Embedded Lossy to Lossless Image Compression," IEEE Trans. On Image Processing, vol. 10, no. 3, pp. 383-392, March 2001.
- [3] P.P. Vaidyanathan, "Multirate Systems and Filter Banks," Prentice Hall Signal Processing Series, 1993.